JOURNAL OF Materials CHEMISTRY

Preparation and properties of silica hybrid gels containing phytic acid

Charles Samba-Fouala,[a] Jean-Charles Mossoyan,[a] Mireille Mossoyan-Déneux,*[a] David Benlian,[a] Corine Chanéac[b] and Florence Babonneau[b]

[a]*Laboratoire de Chimie de Coordination Université de Provence, Centre Universitaire de St Jérôme Case D 22, Avenue de l'Escadrille, Normandie-Niemen, F-13397 Marseille Cedex 20, France. E-mail: Mireille.Mossoyan-Deneux@LCC.u-3mrs.fr*
[b]*Chimie de la Matière Condensée Université Pierre et Marie Curie, 4 Place Jussieu, F-75252 Paris Cedex 05, France*

Received 18th October 1999, Accepted 4th November 1999

Silica–phosphate mixed gels have been prepared by the sol–gel process from tetramethoxysilane and phytic acid (IP_6H_{12}). They contain inositol phosphate ester units anchored by covalent P–O–X bonds (X = P or Si) as isolated polyphytate clusters either embedded or bound in the amorphous network. ^{31}P NMR of the liquid phases at low temperature was used to monitor the initial steps of hydrolysis–condensation reactions at the sol stage. Dried gels have been characterized by ^{13}C, ^{29}Si and ^{31}P MAS NMR, powder X-ray diffraction and FTIR. The ability of these gels to sequestrate metallic ions, such as La^{3+} and Zn^{2+}, on the open phosphate sites has been investigated. The resulting samples undergo structural modifications during the heat treatment which leads to the formation of silica–lanthanum phosphate and silica–zinc pyrophosphate mixtures. The specific influence of the inserted cation on the structure of the final silica–phosphate obtained at 600 and 900 °C is discussed.

1 Introduction

In recent years, the study of phosphate-containing silica, in some instances with inserted transition metals or rare-earth (lanthanide) cations, has attracted much attention. Physical properties of these solids (optical, conducting, luminescence) have led to many applications in the fields of optical fibres, surface coatings, ceramic filters and many more.[1–6]

Among different preparation methods of phosphosilicate glasses, examples include high temperature procedures based on melting of different oxides[7–9] or the use of sol–gel chemistry in which metallic alkoxides [$M(OR)_4$] are reacted with phosphoric acid (H_3PO_4) or alkylphosphates [$PO(OH)_{3-x}(OR)_x$, R = CH_3, C_2H_5,…].[10–12] More recently, phosphate ceramics have been synthesized using the sol–gel route by direct reaction of anhydrous P_2O_5 with metallic alkoxides.[13]

myo-Inositol hexakisphosphoric acid (IP_6H_{12}, phytic acid), with twelve acidic protons on six phosphate ester groups, appears in aqueous solution in either of two conformations: axial or equatorial (Fig. 1) as a result of intramolecular hydrogen bonding between phosphate groups which leads to stabilisation of the equatorial form up to pH 10 and of the axial form at higher pH values.[14] Ionisation constants reported by Brigando *et al.*[14] span a remarkably large range ($0 < pK_a < 12$). The ability of this multifunctional ligand to complex metal cations in acidic media[15,16] is known to be stronger than that of phosphoric acid or of its alkyl derivatives. In the aim to produce a material for sequestering metallic cations and particularly heavy cations which are water polluting, we use phytic acid as the precursor of phosphate sites for the preparation of phosphosilicate gels by the sol–gel route. Because of its structure, phytic acid may be a good catalyst for the hydrolysis of alkoxysilanes and a condensation centre for the subsequent gel-growth. The low temperature maintained during the sol–gel process preserves the organic structure of the phytic acid. As opposed to the silica phosphate gels formed from phosphoric acid or P_2O_5, phosphate groups are organized in space in a specific network induced by the structure of the phytic acid. In this work, we first report on the sol–gel synthesis of a mixed silica–phosphate material using phytic acid as precursor and on the characterization of the obtained gel. Then, we describe its ability to sequestrate metallic cations (Zn^{2+} and La^{3+}) on the phosphate anionic groups which are distributed in the silica network. Zn^{2+} and La^{3+} have been chosen as examples of diamagnetic and redox free cations suitable for NMR experiments in our experimental conditions and as good models for heavy polluting metals.

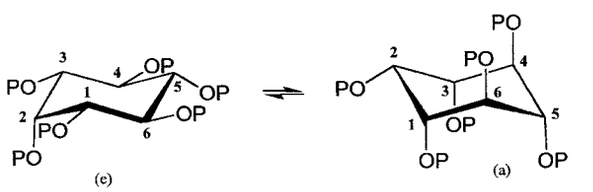

Fig. 1 Equatorial (e) and axial (a) conformations of phytic acid (IP_6). P = $-PO_3H_2$, $-PO_3H^-$ or $-PO_3^{2-}$ depending on pH. The numbering corresponds to cyclohexyl carbons bearing phosphate groups. Each phosphorus atom is labelled with the same number as the carbon to which it is linked.

2 Experimental

2.1 Preparation of phosphosilicate gels

Reactants. Commercial grade tetramethoxysilane (TMOS) (Fluka), and hydrated sodium phytate ($IP_6Na_{12}\cdot 30H_2O$, Aldrich) were used without further purification. Phytic acid solutions were prepared from sodium phytate by ion exchange using a Dowex 50WX4 resin according to a reported method.[14]

Solution studies. In order to study the first stages of the condensation reaction between IP_6 and TMOS in solution, the evolution of the sol was followed by ^{31}P NMR spectroscopy. Studied sols were prepared at 0 °C in order to slow down the reaction, initiated by mixing 1 ml IP_6 solution adjusted at 20 °C

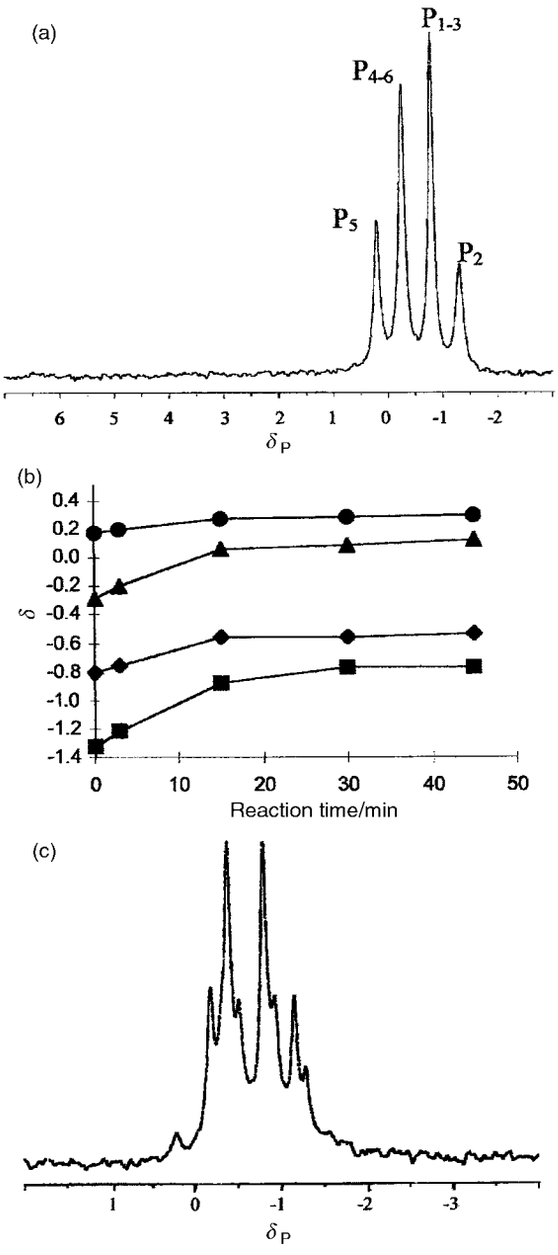

Fig. 2 ^{31}P solution NMR spectra of IP_6/TMOS showing evolution of the sol. (a) Starting IP_6 solution (pH = 3), (b) variation of the chemical shifts of each type of phosphorus with the reaction time [P1,3 (◆), P2 (■), P4,6 (▲), P5 (●)] and (c) ^{31}P solution NMR spectra of IP_6 in the organic (TMOS) phase after a very short reaction time (1 min).

to pH = 3 and 3 ml TMOS (P/Si = 0.05; H_2O/TMOS = 2.5). ^{31}P NMR spectra were recorded at 15 min intervals (Fig. 2). Aqueous IP_6 is not miscible with TMOS so that the reaction starts at the interface. As the reaction proceeds, enough methanol is released to homogenize the mixture. In spite of its low solubility, no precipitation of IP_6 was observed.

In order to study the distribution of IP_6 between the two phases, at the very beginning of the process, a separate sample was adjusted to pH = 1 to further slow down the gelation process. Then TMOS was added in the same proportion as in the first experiment. After stirring for 1 min, the mixture was allowed to settle for 10 s at 0 °C. The aqueous and organic phases were then decanted off and ^{31}P NMR spectra were recorded at −5 °C. Under such conditions, the solution does not change, as revealed by the constancy of spectra recorded after a variety of times of reaction.

Study of the solid phases. The aqueous phytic acid solution was 0.8 M and the pH was adjusted to 0.3. 30 ml of this IP_6 solution was mixed at 0 °C with 10 ml of TMOS and vigorously stirred for 10 min at 0 °C, then left at room temperature under mild stirring. The gelation time was 40–50 min and the obtained gel was translucent, compact but crumbly. This sample, H_{100}, was dried in air at room temperature for 10 h, then at 100 °C for 10 h, and then powdered and dried again at 100 °C for 5 h (P/Si = 0.21). After ageing for a week in a dessicator, sample H_{100} was heated in a furnace in air at 600 °C and one sample was heated at 900 °C for 10 h. This gave samples H_{600} (P/Si = 0.21) and H_{900} (P/Si = 0.032) (P/Si ratios were determined by elemental analysis on the final samples).

Sequestration of metallic cations (Zn^{2+} and Ln^{3+}). The sequestering capacity towards metallic ions was investigated in the following manner: 2 g of gel H_{100}, maintained in a dessicator for three months was suspended in 20 ml of 0.01 M zinc acetate or lanthanum acetate solution (the pH was adjusted to 2 to avoid precipitation of cations). The dispersion was sonicated for 14 min and allowed to equilibrate for 2 h at room temperature. After filtration the gels were dried at 100 °C. Samples with Zn^{2+} and La^{3+} cations are labelled Zn_{100} (P/Zn = 2.6, Si/Zn = 85) and La_{100} (P/La = 3.4, Si/La = 25), respectively. These gels were placed in a furnace maintained at 600 °C for 10 h to yield Zn_{600} (P/Zn = 1.5, Si/Zn = 4.5) and La_{600} (P/La = 3.2, Si/La = 6.7), respectively, while heating at 900 °C for 10 h gave samples Zn_{900} (P/Zn = 1.5, Si/Zn = 4.7) and La_{900} (P/La = 2.5, Si/La = 4.8), respectively.

2.2 Characterization techniques

A Metrohm E605 pH-meter coupled with a EA120 Metrohm combined glass microelectrode was used for pH measurements. The electrode was calibrated by means of standard buffers. The pH of the samples was adjusted to suitable values with ammonia or HCl.

The solution ^{13}C NMR spectra were recorded on a Bruker HX Fourier-transform NMR spectrometer operating at 400 MHz for ^{1}H. MeOH was used as an internal reference, with tetramethylsilane as the chemical shift reference ($\delta 0$). The solution state ^{31}P NMR spectra were recorded on a Bruker ARX 200 Fourier-transform NMR spectrometer operating at 81.01 MHz. ^{31}P chemical shifts were measured relative to an external reference (85% H_3PO_4 in water).

MAS NMR spectra were recorded either on a Bruker MSL400 or a MSL300 spectrometer equipped with magic angle spinning. The ^{31}P NMR spectra were obtained at 162.0 MHz using a 5 mm Doty probe, with spinning rates ranging from 9 to 10 kHz. The acquisition parameters were the following: 1 μs pulse width, 3 s recycle delay. The ^{29}Si NMR spectra were recorded at 79.5 MHz using a 7 mm Bruker probe with a spinning rate of 4 kHz. The pulse width and recycle delays were 2 μs and 60 s, respectively. The ^{13}C NMR spectra (75.5 MHz) were recorded using the cross-polarisation sequence with a contact time of 3 ms. $SiMe_4$ (^{29}Si and ^{13}C) and H_3PO_4 (^{31}P) were used as chemical shift references. The Winfit program[17] was used for the various simulations. FTIR spectra were recorded on a Nicolet 20 SXB spectrometer in the frequency range 400–4000 cm^{-1} using 0.5–1% w/w of the compound in KBr pellets. XRD measurements were performed using a powder diffractometer (Philips PW1830) operating in the reflection mode with Cu-Kα radiation and equipped with a graphite back monochromator. The patterns were analysed using the Philips PC APD 3.5 program package. The effective particle size was calculated applying the Scherrer formula to the line width at half maximum assuming Gaussian profiles for instrumental and experimental broadenings. Elemental analyses were performed at the Service Central d'Analyses du CNRS

(Vernaison, France) by inductive coupling plasma atomic emission spectroscopy.

3 Results and discussion

3.1 Synthesis of phosphosilicate gels

IP_6 as phosphate precursor, has gelation times similar to those of H_3PO_4[7] which has been shown to be a more reactive precursor than phosphate triesters.[18] For H_3PO_4, the short gelation times, compared to those obtained with triethylphosphate (TEP) are attributed to acid catalysis as well to the presence of phosphate ions which play a significant role in activating cleavage of Si–O–C bonds, through the nucleophilic attack of Si, whereas TEP does not interfere in the hydrolysis and condensation of TEOS.[10] In a series of other experiments at variable P/Si ratios and at constant pH, shorter gelation times were obtained at higher P/Si ratios. With a constant starting P/Si ratio, the gelation time decreases when the pH is raised within the acidic range. From a series of experiments at higher pH, we can conclude that the effect of increasing P/Si is higher than that of decreasing the pH. As a phosphate precursor, IP_6 appears to be at least as reactive as H_3PO_4.

Study of the initial sol formation step in solution. Fig. 2(a) shows the ^{31}P spectrum of the starting IP_6 solution at pH = 3. At $1 < pH < 4$, IP_6 adopts an equatorial conformation.[14,19,20] Up to pH = 3.6, the ^{1}H decoupled ^{31}P NMR spectrum shows four peaks, which are very sensitive to pH, with intensity ratio 1 : 2 : 2 : 1 assigned to P5, P4 and P6 (P4,6), P1 and P3 (P1,3), and P2 (see Fig. 1). After mixing with TMOS, ^{31}P NMR spectra are recorded at 15 min intervals. As the reaction proceeds, the peaks broaden and shift. P2 and P1,3 on one hand and P5 and P4,6 on the other become closer and fuse in a two-humped unresolved broad peak. The evolution with time of the chemical shifts of each signal is also shown in Fig. 2. All the ^{31}P peaks are shifted downfield. It is seen that P2 (the only axial phosphate in the equatorial conformation) and P4,6 peaks undergo similar behavior and undergo larger variations than P1,3, whereas P5 shows only a very small shift. 15 min after the onset of the reaction, the chemical shifts of P5 and P1,3 remain nearly constant while those of P4,6 and particularly of P2 still move significantly downfield. Brigando *et al.*[14] have shown that all the ^{31}P chemical shifts of IP_6 move downfield when the pH is raised, as deprotonation of phosphate groups induces deshielding of the corresponding nuclei. One can relate the observed downshift to deprotonation of aqueous phosphate groups when TMOS approaches IP_6 in the sol during the first step of the reaction. As no signal at δ_P *ca.* −10 or −20, assignable to P–O–Si or P–O–P bonds[8] is observed, we conclude that condensation takes place later. (Previous studies of ^{31}P NMR in gels indicate that ^{31}P isotropic chemical shifts become more negative as the degree of polymerization increases.[15,18]) Atom P2 which is more exposed to the medium, undergoes the strongest interactions with surrounding TMOS molecules, more so than between P4 and P6 of IP_6 with TMOS. Atom P5 is not affected by the approach of siloxane side arms: either because it is already deprotonated at the start of the reaction or alternatively remains protonated during the process. Atoms P1 and P3 are more sheltered so that the observed variation in chemical shift is intermediate: this could be interpreted as an attenuated interaction with –Si–O–CH_3 groups attached to P2, P4 or P6, or from free TMOS reacting incompletely because of steric hindrance. The lower reactivity of the P5, P1 or P3 groups would leave pendent protonated phosphate groups.

The second experiment monitored by ^{31}P NMR was performed in the slowest conditions compatible with the recording of spectra, in order to study the behaviour of IP_6 in the aqueous and organic phases during the initial reaction steps. The spectrum of the starting IP_6 solution at pH = 1 before mixing is very similar to the spectrum shown in Fig. 2(a) with four peaks assigned to P5, P4,6, P1,3 and P2 with chemical shifts at δ −0.19, −0.39, −0.81 and −1.16, respectively. The slight modifications of the chemical shifts are due to the different pH used.

The spectrum of IP_6 in the aqueous phase after a very short reaction time with TMOS is also similar to the spectrum in Fig. 2(a). The chemical shifts vary slightly, moving downfield for P5, P4,6, P1,3, and P2 to δ −0.13, −0.34 −0.76, and −1.13, respectively. In aqueous medium, some TMOS has migrated and induces the beginning of deprotonation of IP_6.

The spectrum of the organic phase [Fig. 2(b)] exhibits two superimposed spectra, both typical of IP_6. The more intense spectrum is identical to the initial spectrum before mixing, with the same chemical shifts while the less intense spectrum is slightly shifted upfield. This establishes the immediate diffusion of IP_6 into the organic TMOS phase and its presence as early as the first minute, in two or several slightly altered forms of the free molecule. The upfield shift of the less intense spectrum in the TMOS phase confirms the set-up of the interaction between IP_6 and TMOS in the early stage of the condensation process.

3.2 Characterization of phosphosilicate gels

Elemental analysis of the H_{100} gel gives a P/Si molar ratio of 0.21 showing the presence of phosphorus containing species within the silica network, which is X-ray amorphous. Spectroscopic techniques were thus used to obtain structural information.

MAS NMR study. The ^{13}C MAS NMR spectra of crystalline $IP_6Na_{12}{\cdot}30H_2O$ as reference and of gel H_{100} are shown in Fig. 3(a) and (b), respectively. In Fig. 3(a), a signal at δ *ca.* 73 with a shoulder at lower field is observed and a simulation gives two chemical shifts at δ 73.8 and 67.0, which correspond to the completely deprotonated form of IP_6, according to a ^{13}C study[14] in solution. The main signal at δ 73.8 is assigned to C1,3, C4,6 and C5 while the shoulder at δ 67.0 arises from C_2, the only carbon bearing an axial phosphate in the equatorial conformation of IP_6. The relative intensity of these two peaks is also in fairly good agreement with this assumption. In Fig. 3(b), the broad signal at δ 60–85 is assigned to phytic acid. The shoulder at δ 60–70 can be attributed to a modified C2 carbon such as that found in the deprotonated molecule and confirms the results of the solution ^{31}P NMR studies. The main peak at δ 70–85 is not informative about the state of the other five carbons by reference to free solvated IP_6 as their resonances only change from δ 72 to 78 upon titration with a strong base. The peak detected at δ *ca.* 20 is probably due to

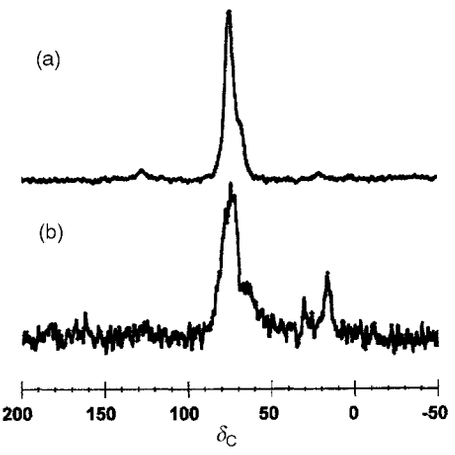

Fig. 3 ^{13}C MAS NMR spectra of (a) crystalline $IP_6Na_{12}{\cdot}30H_2O$ and (b) of the gel H_{100}.

alkyl residues resulting from side products of the condensation reactions. In conclusion, gel H_{100} is shown to be comprised of the cyclohexyl unit of IP_6 with the P2 site modified in a manner similar to the deprotonated state.

The ^{29}Si MAS NMR spectrum of the H_{100} sample is quite similar to that of silica gel,[18] with a main peak at δ *ca.* -110 assigned to a Q^4 unit with a silicon-centred tetrahedron connected to four other silicon tetrahedra[22,23] [*Si*$(OSi)_4$], and a minor component at δ *ca.* -102 assigned to a Q^3 unit,[24,25] [*Si*$(OSi)_3(OZ)$ (Z = H or Me)]. The degree of condensation of the network, which gives the percentage of siloxy groups which have condensed, is close to 90%. The presence of *Si*$(OSi)_2(OP)(OZ)$[18] units expected to lie in the range δ -102 to -112 is postulated as these two peaks are less resolved than in the spectrum of pure silica gels. It is remarkable that no peak at δ -120, assignable to Q^4 units bonded to four phosphate groups, *Si*$(–O–P)_4$,[18] is observed in these samples. The dimensions and geometry of IP_6 appear to prevent the approach of four bulky organic molecules around a single silicon atom.

Fig. 4 shows the ^{31}P solid state MAS NMR spectra of the samples H_{100} and H_{600} together with the spectrum of crystalline $IP_6Na_{12}\cdot 30H_2O$. The spectrum for $IP_6Na_{12}\cdot 30H_2O$ [Fig. 4(a)] shows a characteristic peak at δ 6.9 due to the phosphate side groups, PO_3^{2-} in unprotonated IP_6^{12-} molecules. The spectrum of sample H_{100} [Fig. 4(b)] shows a broad signal with three peaks at δ -0.5, -10.6 and -21.0 with relative intensities 27 : 32 : 41. As ^{31}P chemical shifts in glasses become more negative as the degree of condensation of the network increases,[18,21] they are assigned as Q'^0, Q'^1 and Q'^2 phosphate sites,[10,11,18,26] respectively, where Q'^n refers to a phosphate group bound to *n* silicon atoms or to *n* phosphorus atoms through P–O–X bonds.[10] The peak at δ -0.5 is in the range of pure phytic acid ^{31}P resonances >CH–O–P=O$(OH)_2$, (Q'^0), as shown by the solution state study and assigned to free IP_6 molecules, simply adsorbed in the host silica or encapsulated in siloxane cages or to pendent protonated phosphate groups belonging to phytic acid molecules bound to the silica host network only by one or a few of their phosphate groups. It is unlikely that they correspond to free O=P$(OH)_3$ groups resulting from the partial hydrolysis of a fraction of IP_6.[27] Hydrolysis of IP_6 leading to a mixture of inositol and mono-, bis-, tris-, tetrakis- or penta-phosphates is difficult, incomplete and takes place at much higher temperatures under more drastic conditions. The second peak at δ -10.6 is assigned in the literature[10,11,18] to singly bound Q'^1 species: O=P$(OH)_2$(O–X–O–) or in our case to >CH–O–P=O(OH)(O–X–O–) (X = Si, P). These results show that many phytic acid molecules either are covalently bonded to the silica network or are polymerized, forming oligophytate clusters through P–O–P bonds. Sample H_{600} [Fig. 4(c)] is characterized by a broad, slightly non-symmetric signal with two components at δ -26.7 and -37 with relative intensities of 7 and 93%. They are assigned to Q'^2 and Q'^3 species, respectively, with a large majority of Q'^3 sites [O=P$(O–X–O–)_3$]: this is in agreement with the decomposition of the inserted inositol species and a better cross-linking at the phosphorus sites at high temperature. Sample H_{900} shows a very weak ^{31}P signal which reveals the loss of phosphorus during heat treatment between 600 and 900 °C.

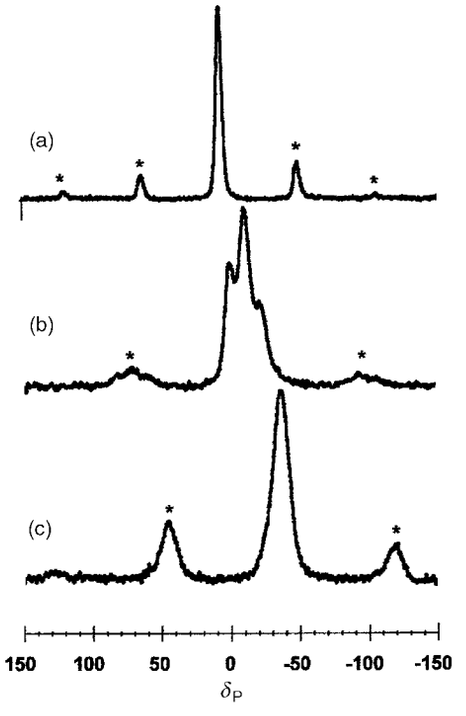

Fig. 4 ^{31}P MAS NMR spectra of the prepared silica–IP_6 gels. (a) Crystalline $IP_6Na_{12}\cdot 30H_2O$, (b) sample H_{100} and (c) sample H_{600}.

FTIR study. The spectrum of sample H_{100} [Fig. 5(a)] is very similar to that of a pure silica gel with bands at 467 cm^{-1} [δ(Si–O–Si)], 569 cm^{-1} (as a shoulder of the band at 467 cm^{-1}), 799 cm^{-1} (symmetric O–Si–O stretches), 966 cm^{-1} (SiO_4 stretch perturbed by the presence of a neighbouring atom other than Si) and 1100 cm^{-1} (O–Si–O asymmetric stretches). As already reported for phosphosilica gels[7] these bands are intense and overlap the phosphate bands at *ca.* 500 cm^{-1} for PO_4^{3-} and 780 cm^{-1} for P–O–P bonds, from 900 to 1035 cm^{-1} for $P–O^-$ bond stretching and at 1260 cm^{-1} for P=O double bond stretching.[28]

In H_{600}, [Fig. 5(b)] some differences are of note upon comparison with H_{100}. The bands at 467 and 569 cm^{-1} become a broad band at 486 cm^{-1}. A new double broad band appears between 642 and 678 cm^{-1} which does not occur in SiO_2, but is described in the literature[12] as a phosphate O=P–O bending vibration, which is very sensitive to the size of bonded cations. The large peak around 1100 cm^{-1} (Si–O–Si stretching) has a modified profile and covers the band at 966 cm^{-1}. This has been described elsewhere as the result of the transformation of low temperature (300 °C) amorphous phosphosilica coatings to more crystalline phosphosilicas at higher temperature (750 °C).[5] Shoulders at 1325 and *ca.* 1200 cm^{-1} appear on

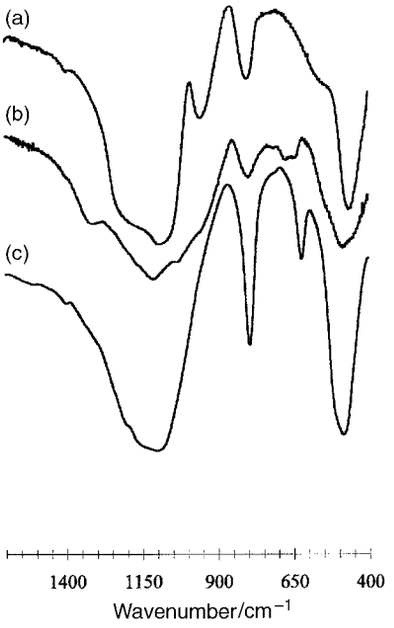

Fig. 5 IR spectra for samples H_{100} (a), H_{600} (b) and H_{900} (c).

the broad Si–O, P–O peak and are likely due to the P=O stretching of phosphates.[26] In H_{600} all the bands are broad and in H_{900} [Fig. 5(c)], the same modifications are observed but the bands are sharper, particularly the double broad band, between 642 and 678 cm^{-1}, ascribed to a phosphate O=P–O bending vibration, which is now a single sharp medium band at 620 cm^{-1}.

Proposed structure for the phosphosilicate gel. The ^{13}C MAS NMR spectrum confirms the insertion of IP_6 in the dried gel. The ^{29}Si MAS NMR spectrum shows a highly condensed network based on Q^3 and Q^4 sites. This important degree of crosslinking at the silicon atoms, and the large proportion of phosphorus atoms of Q^1 and Q^2 type show that condensation reactions have taken place on silicon and phosphorus atoms. The ^{29}Si and ^{31}P MAS NMR spectra of the gels dried at 100 °C suggest homocondensation P–O–P and Si–O–Si with the formation of silicate and oligophytate species in a heterogeneous gel. However the ^{29}Si MAS NMR spectrum does not exclude the existence of some Si–O–P bonds between discrete silicate and clustered phytate regions. The existence of many Q^0 phosphates in the gels preserves the sequestering properties of phytic acid in its inserted form. Fig. 6 shows an illustration of a possible structure of the gels formed in our experimental conditions.

3.3 Sequestration of metallic cations (Zn^{2+} and La^{3+})

X-Ray diffraction results. The XRD study shows that all the samples dried at 100 °C are amorphous. At 600 °C, Zn_{600} shows an XRD pattern with peaks characteristic of zinc pyrophosphate, γ-$Zn_2P_2O_7$ (JCPDS file 43-0488) on top of a broad background typical of an amorphous phase. Sample La_{600} shows a higher crystallinity, with peaks due to lanthanum phosphate, $LaPO_4$ (JCPDS file 32-0493). The diffraction pattern of La_{900} shows a unique phase of lanthanum phosphate (Fig. 7) while that of Zn_{900} is a superimposition of cristobalite and zinc pyrophosphate, β-$Zn_2P_2O_7$ (JCPDS file 8-0238). For comparison, the XRD pattern of H_{900} is characteristic of a well crystallized phase of cristobalite: indeed the ^{31}P NMR study has suggested that most of the phosphorus atoms have been lost during pyrolysis, being released as P_2O_5. Formation of $LaPO_4$ and $Zn_2P_2O_7$ phases shows the efficiency of the H_{100} gel to trap both cations. From XRD data, the dimensions of the metal phosphate particles were estimated from which a size of 60 nm for $LaPO_4$ was obtained with good reliability as there

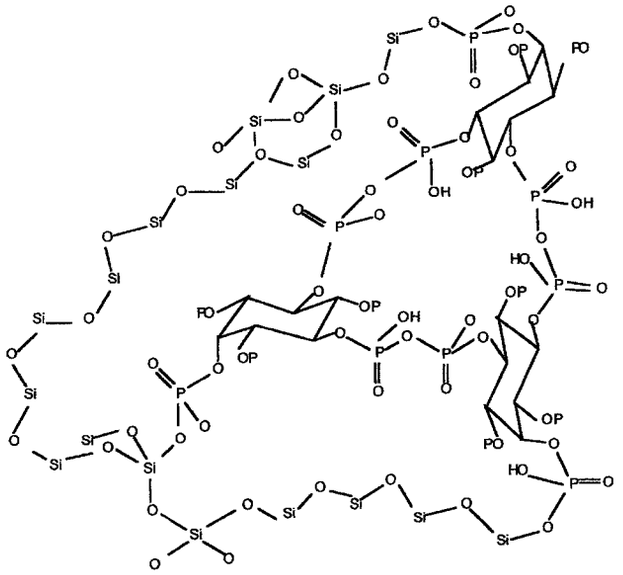

Fig. 6 Illustration of a possible structure of the gel H_{100}.

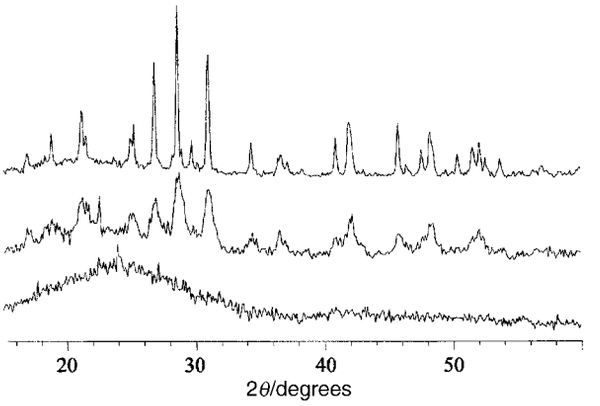

Fig. 7 X-Ray diffraction patterns of gels La_{100} (a), La_{600} (b) and La_{900} (c).

are many lines. For $Zn_2P_2O_7$ the estimation is more difficult since there are few lines in superimposition with the diffraction pattern of cristobalite; an estimation indicated the dimensions of the particles to be *ca.* 100 nm.

FTIR spectra. Fig. 8 and 9 show the FTIR spectra of Zn_{100}, Zn_{600}, Zn_{900} and La_{100}, La_{600}, La_{900}, respectively. Spectra for samples Zn_{100} and La_{100} are very similar to the spectrum of H_{100}. A sharp medium sized band around 620 cm^{-1} undetected in the low temperature dried gels appears in all samples at 600 and 900 °C, even in H_{900}. We assign this band to a phosphate O=P–O bending vibration, modified by the presence of P–O–Si and/or P–O–P bonds. The influence of inserted metallic ions is more striking in the annealed samples, with the presence of some new small bands (at 589 cm for Zn_{600}; at 580 cm^{-1} and a shoulder at 535 cm^{-1} for La_{600}, and at 538, 564, 578 cm^{-1} for La_{900}). These bands, which appear very strong in the same region in zinc phytate or phosphate, and lanthanum phytate or phosphate, are ascribed to metal bonded phosphate bending modes O=P–O or O–P–O.[11,12,29] They are not present in spectra recorded on samples without phytic acid, such as pure SiO_2 gels reacted with a Zn acetate solution and heated to 600 °C (the sequestration of ions by the phosphate groups on IP_6 induces no evident changes in the 100 °C spectra). Metal–phosphate persists and induces important modifications in the bending modes of phosphate groups at 600 °C, when the inositol rings have been decomposed. The similarity of our La_{600} spectrum with the IR spectrum of microcrystalline $LaPO_4$ gel synthesized by Guo *et al.*[12] in ethanol and dried

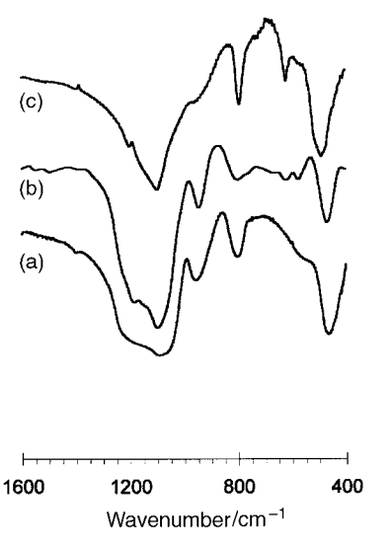

Fig. 8 IR spectra of Zn_{100} (a), Zn_{600} (b) and Zn_{900} (c).

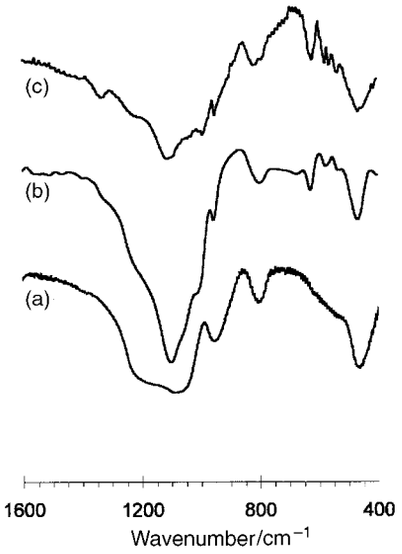

Fig. 9 IR spectra of La_{100} (a), La_{600} (b) and La_{900} (c).

under vacuum is remarkable. By comparison to their published spectrum, only two additional absorptions are present (at 472 and 804 cm^{-1}) which are assigned to O–Si–O bending modes. Subsequent heating to 900 °C modifies the spectra in the region of the metal-dependent vibrations. The band at 589 cm^{-1} is almost absent for Zn_{600} while for La_{600}, the bands at 580 and 535 cm^{-1} split into three bands at 538, 564 and 578 cm^{-1}.

MAS NMR study. The ^{31}P MAS NMR spectra of Zn_{100}, Zn_{600}, Zn_{900} and La_{100}, La_{600}, La_{900} are shown in Fig. 10 and 11, respectively. For Zn_{100} and La_{100}, the peaks are broader than those in the annealed compounds and confirm the transformation of amorphous phosphosilicate gels to crystalline phosphosilicates at higher temperature,[7] as shown by the XRD study. The spectrum of Zn_{100} [Fig. 10(a)] is similar to that of H_{100} [Fig. 4(b)]. By contrast, Zn_{600} presents a clearly different spectrum [Fig. 10(b)]. The Q'^0 peak is reduced and the Q'^2 peak virtually disappears. Peaks ascribed to Q'^0 and Q'^1 species become sharper and better resolved with a splitting of the Q'^1 peak into two peaks at δ *ca.* −7 and −10. At 900 °C [Fig. 10(c)], the Q'^0 peak virtually disappears and the peak at δ −7 is reduced somewhat. There is no peak at δ *ca.* −10 but a new group of three peaks appears in the Q'^2 region at δ −16, −19 and −21. It is remarkable that Q'^2 species are present at 100 °C, and disappear at 600 °C probably as a consequence of decomposition of –CH–O–P bonds, as well as some P–O–P bonds. At 900 °C, new signals are observed owing to the formation of zinc pyrophosphate. No Q'^3 species are detected which suggests that all the P atoms are part of the pyrophosphate phase. The ^{29}Si MAS NMR spectrum of Zn_{900} [Fig. 12(b)] shows a sharp peak at δ −110 similar to that found in H_{900} [Fig. 12(a)] characteristic of crystalline cristobalite in accord with the XRD data.

The final product, Zn_{900}, can thus be described as a mixture of crystalline zinc pyrophosphate and cristobalite; the presence of an amorphous phase of phosphosilicate as a minor component can not be excluded, but is not clearly detected in the NMR spectra.

In contrast to the Zn system, the introduction of La^{3+} considerably changes the ^{31}P MAS NMR spectrum of the gel [Fig. 11(a)] with the appearance of two broad signals at δ −0.8

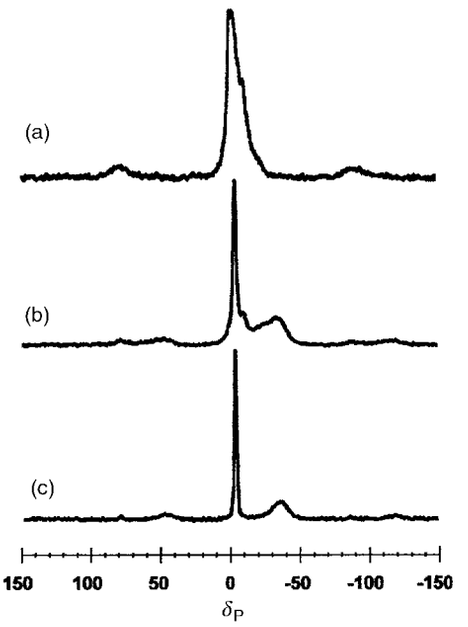

Fig. 11 ^{31}P solid state MAS NMR spectra of compounds La_{100} (a), La_{600} (b) and La_{900} (c).

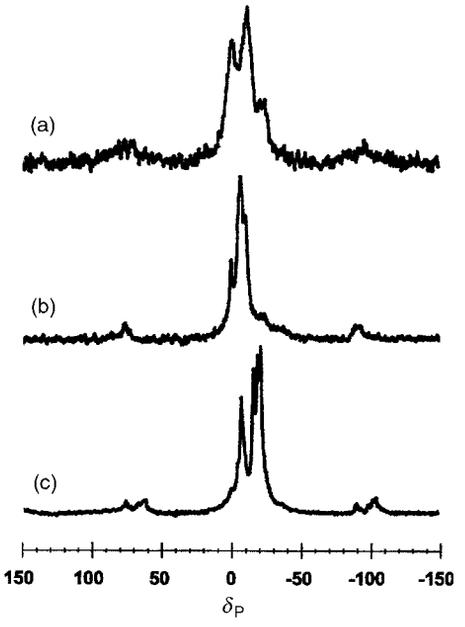

Fig. 10 ^{31}P solid state MAS NMR spectra of compounds Zn_{100} (a), Zn_{600} (b) and Zn_{900} (c).

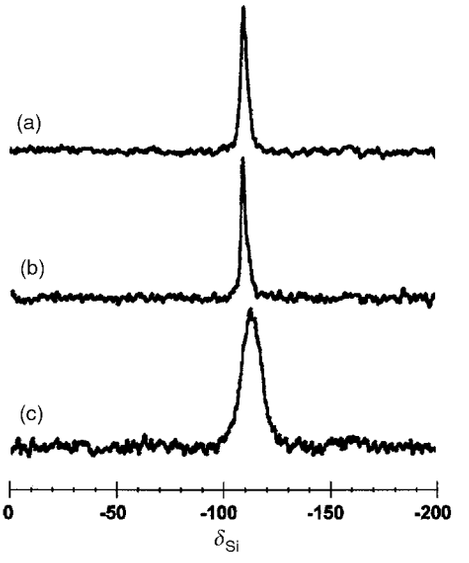

Fig. 12 ^{29}Si MAS NMR spectra of compounds H_{900} (a), Zn_{900} (b) and La_{900} (c).

and −2.9. At 600 °C [Fig. 11(b)] the spectrum is very different from that observed for H_{600} with a sharp peak at δ −4.3 and with a small shoulder at δ −10.0. The peak at δ −4.3 is similar to that observed by Guo *et al.* for $LaPO_4$.[12] Additionally, a small asymmetric signal centred at δ −33.3 is still present, similar to that observed for H_{600} and assigned to Q'^2 and Q'^3 sites. At 900 °C, only two peaks remain, a sharp signal at δ −4.4 due to $LaPO_4$ and a broad signal centred at δ −37.8, due to Q'^3 species (a peak at δ −38.3 is reported as clearly characterising a P–O–Si linkage[13]). While the XRD results for La_{900} have revealed the presence of only one crystalline phase, $LaPO_4$, the ^{29}Si MAS NMR spectrum [Fig. 12(c)] shows a broad signal centred at δ −113 characteristic of the presence of an amorphous phase. This signal is shifted compared to that for silica suggesting the presence of a phosphosilicate phase in agreement with the ^{31}P NMR results. The final product, La_{900} can thus be described as a mixture of crystalline lanthanum phosphate and a residual amorphous phosphosilicate phase.

From the ^{31}P and ^{29}Si MAS NMR and FTIR spectra, we can conclude that in the starting gels, the La^{2+} cations influence the environment of the phosphate groups of the phytic acid molecules to a greater extent than the Zn^{2+} cations. However, at 600 °C, both cations appear bonded to the phosphate groups after decomposition of the organic groups, and crystalline phosphate phases start to crystallize, as shown by XRD.

4 Conclusion

IP_6 appears to be at least as reactive as H_3PO_4 for the preparation of phosphosilicate gels *via* the sol–gel route. The study of the sol-to-gel transformation as monitored by ^{31}P NMR establishes the immediate diffusion of IP_6 into the organic TMOS phase and the early setup of the interaction between IP_6 and TMOS in condensation, this interaction occurring on P2, then on P4 and P6. Atom P5 is not affected by the approach of siloxane, thus leaving a number of free phosphate anions available for cation sequestration.

A solid state ^{13}C MAS NMR study establishes the insertion of the cyclohexyl moieties of IP_6 in the gel network. The absence of direct evidence for the presence of P–O–Si bonds in the gels is in favour of homocondensation reactions with the formation of a highly condensed silica network and oligophytate species in a heterogeneous gel. However, the ^{29}Si MAS NMR spectrum does not exclude the existence of some Si–O–P bonds between discrete silicate and clustered phytate regions. The existence of a large number of Q'^0 phosphate species in the gel preserves the sequestering properties of phytic acid in its inserted form. X-Ray diffraction studies indicate the amorphous state of the dried gels and their transformation into cristobalite at 900 °C, in accord with the FTIR spectra. A large loss of phosphorus occurs between 600 and 900 °C as revealed by elemental analysis.

This gel, in contact with zinc acetate or lanthane acetate solution, can trap zinc or lanthanum cations. XRD, FTIR and MAS NMR (^{31}P and ^{29}Si) studies performed on samples heated to 600 and 900 °C, clearly show the formation of zinc and lanthanum phosphate phases. The sequestering property of phytic acid in solution is thus retained in these hybrid gels and could be applied for the treatment of water polluted by heavy metals. This attempt to create hybrid solids able to fix metallic cations under mild conditions and to keep them trapped during drastic thermal treatment is thus successful. The range of temperature between 100 and 250 °C under suitable conditions to retain the organic component should be investigated to study cation rich materials quenched before total migration and condensation takes place. Such materials should display the properties of the cations in the dispersed state, which are not evident by strong interactions in tightly crystalline, high temperature phases: *e.g.* fluorescence, ionic or electronic conduction, magnetic properties. Such microparticulate well formed Zn and La phosphates imbedded in cristobalite (Zn) or in amorphous phosphosilica (La) described here open the way to many more examples of mixtures with other elements.

References

1 A. L. G. Carter, M. G. Sceats, S. B. Poole, P. Y. Timbrell and J. V. Hanna, *J. Non-Cryst. Solids*, 1994, **175**, 71.
2 S. Zemon, G. Lamber, W. J. Miniscallo and A. Thompson, *Proc. SPIE, Int. Soc. Opt. Eng.*, 1991, **1581**, 91.
3 O. Lumholt, T. Rasmussen and A. Bjarxlev, *Electron. Lett.*, 1993, **29**, 495.
4 I. M. Batyaev and I. V. Golodova, *Opt. Spektrosk.*, 1993, **75**, 69.
5 B. I. Lee, Z. Cao, W. N. Sisk, J. Hudak, W. D. Samuels and G. J. Exarhos, *Mater. Res. Bull.*, 1997, **32**, 1285.
6 Z. Cao, B. I. Lee, W. D. Samuels and G. J. Exarhos, *J. Appl. Phys.*, 1998, **83**, 2222.
7 K. B. Langille, D. Nguyen, J. D. Bernt, D. E. Veinot and K. Murthy, *J. Mater. Sci.*, 1993, **28**, 4175.
8 H. Ebendorff-Heidepriem, W. Seeber and D. Ehrt, *J. Non-Cryst. Solids*, 1993, **163**, 74.
9 K. Vivekanandan, S. Selvasekarapandian and P. Kolandaivel, *Mater. Chem. Phys.*, 1995, **39**, 284.
10 C. Fernandez-Lorenzo, L. Esquivias, P. Barboux, J. Maquet and F. Taulelle, *J. Non-Cryst. Solids*, 1994, **176**, 189.
11 B. I. Lee, W. D. Samuels, L.-Q. Wang and G. J. Exarhos, *J. Mater. Res.*, 1996, **11**, 134.
12 Y. Guo, P. Woznicki, A. Barkatt, E. E. Saad and I. G. Talmy, *J. Mater. Res.*, 1996, **11**, 639.
13 Z. Cao, B. I. Lee, W. D. Samuels, L.-Q. Wang and G. J. Exarhos, *J. Mater. Res.*, 1998, **13**, 1553.
14 C. Brigando, J. C. Mossoyan, F. Favier and D. Benlian, *J. Chem. Soc., Dalton Trans.*, 1995, 575.
15 C. J. Martin and W. J. Evans, *J. Inorg. Biochem.*, 1986, **28**, 39.
16 F. Conti, M. Delfini, F. Scorpinaro and U. Croatto, *Inorg. Chim. Acta*, 1987, **140**, 355.
17 D. Massiot, H. Thiele and A. Germanus, *Bruker Rep.*, 1994, **140**, 43.
18 S.-P. Szu, L. C. Klein and M. Greenblat, *J. Non-Cryst. Solids*, 1992, **143**, 21.
19 J. Courtois and M. Masson, *Bull. Soc. Chim. Biol.*, 1950, **32**, 314.
20 L. F. Johnson and M. E. Tate, *Can. J. Chem.*, 1969, **47**, 63.
21 R. K. Brow, R. J. Kirkpatrick and G. L. Turner, *J. Non-Cryst. Solids*, 1990, **116**, 39.
22 K. A. Smith, R. J. Kirkpatrick, E. Oldfield and D. M. Henderson, *Am. Mineral.*, 1983, **68**, 1206.
23 E. Lippmaa, M. Mägi, A. Samoson, G. Engelhardt and A. R. Grimmer, *J. Am. Chem. Soc.*, 1980, **102**, 4889.
24 G. E. Maciel and D. W. Sindorf, *J. Am. Chem. Soc.*, 1980, **102**, 7606.
25 E. Lippmaa, A. V. Samoson, V. V. Beri and Y. I. Gorlov, *Dokl. Akad. Nauk SSSR*, 1981, **259**, 403.
26 D. C. Douglass, T. M. Ducan, K. L. Walker and R. Csencsits, *J. Appl. Phys.*, 1985, **58**, 197.
27 P. Xu, J. Price, A. Wise and P. J. Agette, *J. Inorg. Biochem.*, 1992, **47**, 119.
28 E. E. Khawaja, S. M. A. Durrani, F. F. Al-Adel, M. A. Salim and M. Sakhawat Hussain, *J. Mater. Sci.*, 1995, **30**, 225.
29 A. C. Chapman and L. E. Thirwell, *Spectrochim. Acta*, 1964, **20**, 937.

Paper a908289a